ResearchGate

See discussions, stats, and author profiles for this publication at: https://www.researchgate.net/publication/255766169

3d localization and diffusion of proteins in polyelectrolyte multilayers

ARTICLE *in* SOFT MATTER · NOVEMBER 2012

Impact Factor: 4.03 · DOI: 10.1039/C2SM26500A

CITATIONS
17

READS
33

7 AUTHORS, INCLUDING:

Stephan Schmidt
Max Planck Institute of Colloids and Interfa…
52 PUBLICATIONS **767** CITATIONS
SEE PROFILE

Juergen Rose
Universität Potsdam
5 PUBLICATIONS **62** CITATIONS
SEE PROFILE

Dmitry Volodkin
Fraunhofer Institute for Biomedical Engine…
77 PUBLICATIONS **2,710** CITATIONS
SEE PROFILE

Available from: Dmitry Volodkin
Retrieved on: 25 January 2016

Soft Matter

Dynamic Article Links

Cite this: *Soft Matter*, 2012, **8**, 11786

www.rsc.org/softmatter

COMMUNICATION

3d localization and diffusion of proteins in polyelectrolyte multilayers†

Katja Uhlig,[a] Narayanan Madaboosi,[ab] Stephan Schmidt,[b] Magnus S. Jäger,[a] Jürgen Rose,[c] Claus Duschl[b] and Dmitry V. Volodkin*[a]

Received 28th June 2012, Accepted 11th October 2012
DOI: 10.1039/c2sm26500a

The interaction of diverse biomaterials with surfaces is more crucial than ever for biomedical applications to ensure efficiency and reproducibility. Very interesting surface materials are micrometer-thick polyelectrolyte multilayers. Not only their surface but also the bulk can be loaded with biomaterials like proteins or DNA for various purposes. Therefore, we established a method to analyze the lateral and vertical distribution of fluorescently labelled proteins of various size and charge in polyelectrolyte films composed of poly(L-lysine) and hyaluronic acid by confocal laser scanning microscopy. This approach enables us to measure the diffusion coefficients of the proteins *via* fluorescence recovery after photobleaching as a function of their vertical position in the film and facilitates the understanding of molecular interactions in the film with a high resolution in both space and time. As a result, we confirm that protein loading in the film is driven by electrostatic interactions – uncharged dextran molecules of 10 and 500 kDa do not diffuse into the film. Proteins of different sizes (3–11 nm) can diffuse relatively fast (D = 2–4 μm^2 s^{-1}) independent of their net charge, indicating complex interpolymer interactions. This approach is a new powerful experimental tool to design the polyelectrolyte multilayers for bio-applications by finding a relationship between intermolecular interactions and mobility and availability of biomolecules to biological samples (*e.g.* cells) or detection units (*e.g.* biosensors).

Surface modification in general is of crucial importance in tissue engineering, controlled drug release and implants.[1,2] Biological samples interact with artificial interfaces and this determines the success of such biomedical applications.[3,4] Surface coating in particular not only provides control over cell–surface interactions, but offers additional benefits through its bulk properties. Loading this bulk with specific molecules enables us to influence biological samples if these molecules are released for targeted action. Examples comprise activating cell signaling pathways[5] for cell differentiation,[6,7] cell adhesion and migration,[8,9] proliferation,[10,11] transfection[12] and others.

Polyelectrolyte multilayers (PEM) made from biopolymers[13,14] provide a perfect tool for such advanced applications.[15–18] Due to the film thickness of up to micrometers,[13,19] they exhibit a high loading capacity for biomolecules, which can be used to address cells.[20–26] To fully exploit the reservoir properties of PEMs[27] and to study the availability of molecules, detailed knowledge about the distribution and mobility of molecules inside the films is indispensable. Until now, imaging of PEMs, *e.g.* by confocal laser scanning microscopy (CLSM),[13,19,21,28] only allowed for investigation of lateral diffusion of molecules in the film.[28–32] This is because CLSM has a much lower optical resolution along the optical axis (z axis) than laterally in the plane of flat PEM films (x and y plane) due to the non-spherical shape of the focal volume. In addition, conventional confocal scanning of PEMs allows only for slow recording due to long scanning times and suffers from signal loss due to bleaching. Therefore, we developed here a method which enables monitoring the spatial distribution of fluorescently labelled compounds in a PEM coated on a cylindrical glass fiber. In contrast to standard techniques, this allows for a highly resolved side view (cross-sectional profile) into the PEMs and for a 3d analysis of molecular diffusion by fluorescence recovery after photobleaching (FRAP). Moreover, due to the 90 degrees tilting of the PEMs, diffusion into and inside the films can be followed using the faster scanning axis (x) of a CLSM.

We deposited the polymers on the surface of a cylindrical glass fiber (diameter 100 μm), instead of using a commonly flat surface (Fig. 1a). The PEM coating was carried out by alternately dipping the fibers into poly(L-lysine) (PLL) and hyaluronic acid (HA) at 37 °C for 24 cycles, thus obtaining film thicknesses of (14 ± 5) μm. Film preparation at 37 °C leads to thicker films in comparison to coatings produced at room temperature (~22 °C).[14,33,34] However, the Young's moduli derived by AFM measurements using a colloidal probe show comparable stiffness and therefore comparable density of films prepared at room temperature (43 ± 10) kPa[18] and at 37 °C (63 ± 3) kPa. The coated fibers were laid sidewards on a glass support, such that their long axis (y) was in the plane of the microscopy table, and then incubated with the molecules of interest. Scans of the lower half of the fibers show the homogeneous polymer film (Fig. 1b and c). Because of the round shape of the fiber, both the x and z axes provide the same film profile (Fig. 1c). In all experiments described below, the fibers were only imaged at a height z equal to their radii, to obtain a cross-section of the film perpendicular to the

[a]*Fraunhofer Institute for Biomedical Engineering, Am Mühlenberg 13, 14476 Potsdam-Golm, Germany. E-mail: Dmitry.Volodkin@ibmt.fraunhofer.de*
[b]*Max Planck Institute of Colloids and Interfaces, Am Mühlenberg 1, 14476 Potsdam-Golm, Germany*
[c]*University of Potsdam, Institute for Biochemistry and Biology, Karl-Liebknecht-Str. 24-25, 14476 Potsdam-Golm, Germany*

† Electronic supplementary information (ESI) available: Experimental procedure and schematic view of the microchannel design. See DOI: 10.1039/c2sm26500a

This journal is © The Royal Society of Chemistry 2012

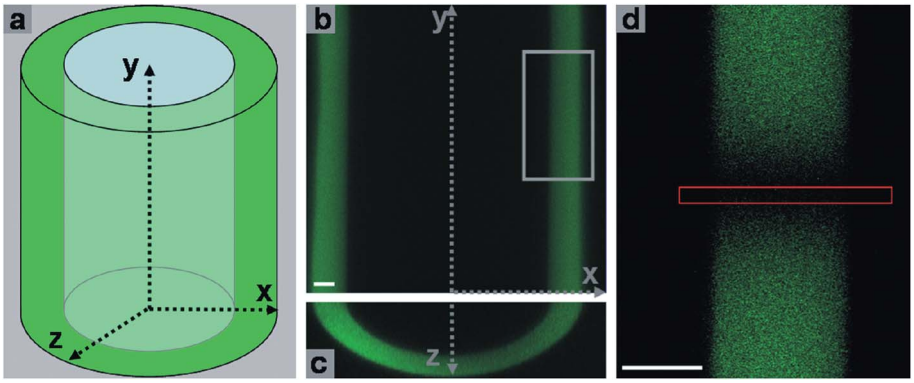

Fig. 1 (a) Sketch of the fiber (blue, diameter 100 μm) coated with $(HA/PLL)_{24}$ film. z is the optical axis of the microscope. (b) Confocal cross-section in the middle of a coated fiber incubated with fluorescein (green). Gray box indicates the area used in FRAP experiments. (c) Orthogonal cross-section. (d) Zoom into the area indicated in (b). The photobleached area (red box) has a width y of 2 μm (contrast enhanced). Scale bars 10 μm.

surface. To measure the mobility of molecules in the film, we bleached a volume extending mainly along the x axis (Fig. 1d) and followed the fluorescence recovery with time (FRAP). This approach overcomes the poorer optical resolution of z slicing, increases the imaging speed with which molecules are traced in the PEMs and thus reduces inadvertent bleaching.

In order to better understand the interaction of bioactive molecules with PEMs, we incubated the film with different FITC-labelled proteins and polysaccharides. The analyzed proteins (papain, lysozyme, bovine serum albumin (BSA), lactalbumin and catalase) differ in hydrodynamic radius (R_0) and surface charge. Fluorescein and dextrans were also used to investigate film interaction with small charged dyes and uncharged macromolecules, respectively.

After 45 min of incubation, all proteins except for BSA entered the film and were homogenously distributed throughout the film (Fig. 2a and S1†). In the case of BSA (Fig. 2f), the protein molecules were only found near the surface of the polymer film where they remained without diffusing into it for at least 60 s. Also, neither of the dextrans tested entered the film, independent of whether they were sized like small proteins (1.9 nm at 10 kDa) or bigger than proteins (15.9 nm at 500 kDa).[35] The difference in diffusion of proteins and dextrans into the film suggests that the transport of macromolecules into the film is mainly driven by electrostatic interactions with components of the polymer film. This is supported by the fact that subsequent to protein incubation, a very low amount of the macromolecules was washed from the film by rinsing (Fig. S1†). To analyze this further, we next studied diffusion of proteins and fluorescein in the film as a function of molecular size and charge. This permits us to conclude about interactions between components of the polymer film and the molecules loaded into it.

The diffusion coefficient D of these molecules was determined from the recovery of fluorescence intensity I over time t. Representative recordings are shown in Fig. 2 for lysozyme (a–e) and BSA (f–j). Following the algorithm of Seiffert and Oppermann, the intensity I across the bleached line is approximated by a Gaussian of width $w(t)$. Then, for any distance d from this line:[36]

$$I(t,d) = I_0 - A(t)e^{-\frac{d^2}{4Dt}} = I_0 - A(t)e^{-\frac{d^2}{2w^2}} \Rightarrow w^2 = 2Dt \quad (1)$$

where I_0 denotes the fluorescence intensity before bleaching ($t \to 0$) and $A(t)$ is a function of time, the amount M of fluorophores destroyed by bleaching and the diffusion coefficient D. This approach considers the initial width of the bleached line to be much thinner than w, so that no assumptions are required concerning the profile of the bleaching beam. An alternative derivation of the expression for the more realistic case of a diffusion back into a rectangular bleaching zone of finite size and for 1d, 2d and 3d diffusion is given in the ESI.† The global diffusion coefficient was estimated by measuring fluorescence intensity profiles along the whole PEM or parts of it every two seconds, averaging, fitting to a Gaussian and calculating the squared half width w^2 of the intensity minimum at every time point (Fig. 2k and l). In accordance with eqn (1), plotting of w^2 as a function of time t results in a straight line with a slope of $2D$ (insets of Fig. 2k and l). Analyzing lysozyme diffusion using the Seiffert algorithm yields $D = (4.4 \pm 0.3)$ μm^2 s^{-1}. If we alternatively assume an initially homogeneously bleached stripe instead of a Gaussian profile, the temporal intensity distribution across it becomes:

$$I(x,t) = I_2 - \frac{I_2 - I_1}{2}\left[\mathrm{erf}\left(\frac{x+x_0}{2\sqrt{ta}}\right) - \mathrm{erf}\left(\frac{x-x_0}{2\sqrt{ta}}\right)\right] \quad (2)$$

where the width of the bleached stripe extends from $-x_0$ to $+x_0$, I_1 is the intensity inside and I_2 is the intensity outside the stripe immediately after bleaching, *i.e.* at $t = 0$ (see ESI†). The diffusion coefficient then is $D = a^2$, yielding $D = (4.6 \pm 0.4)$ μm^2 s^{-1}. Both models, therefore, agree well.

Due to the experimental set-up, not only the global diffusion can be determined, but also the diffusion in different vertical positions inside the film. For that, the cross-section of the film was divided into six zones of 2 μm width and D was calculated for each of them (Fig. S2†). The diffusion coefficients thus obtained from different vertical positions in the film were basically indistinguishable (Fig. S2†). This is in accordance with the homogeneous protein distribution evidenced above.

Table 1 summarizes the estimated diffusion coefficients (D), isoelectric points (PI) and hydrodynamic radii (R_0) of the molecules evaluated. Papain and lysozyme are both positively charged proteins, but papain is 2.2 times larger than lysozyme. Their measured diffusion coefficients differ accordingly: lysozyme diffuses 2.0 ± 0.3 times faster ((4.4 ± 0.3) μm^2 s^{-1}) than papain ((2.2 ± 0.2) μm^2 s^{-1}).

This tendency is not found for negatively charged proteins. Molecular size also does not correlate directly with D: catalase is significantly larger than papain or lysozyme and more than three times larger than lactalbumin, which has the same charge as catalase.

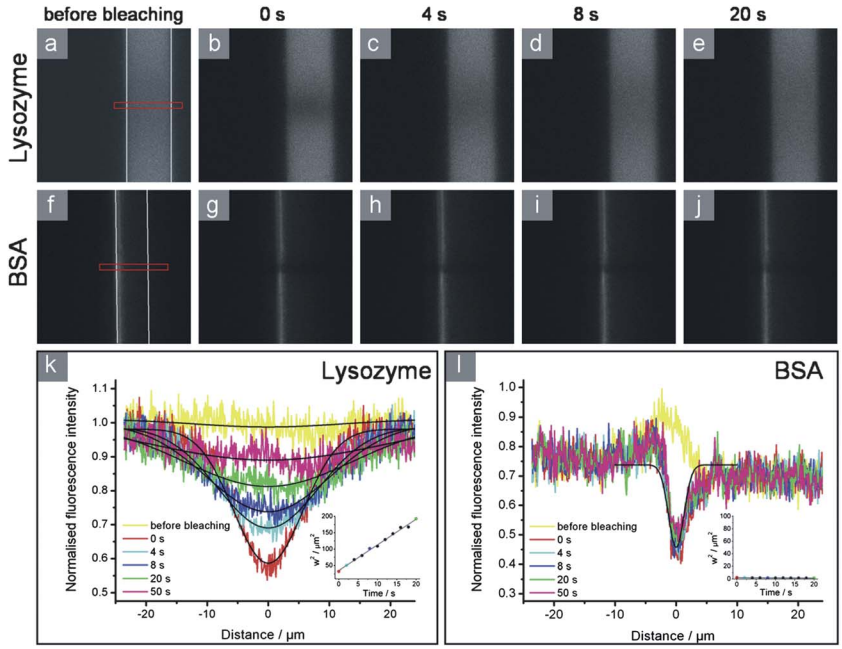

Fig. 2 Time sequence of confocal microscope images for FRAP analysis with $(HA/PLL)_{24}$ film containing FITC-labelled lysozyme (a–e) or BSA (f–j). Distribution of proteins before bleaching shown in (a) and (f). Red boxes highlight the area of bleaching (2 µm) and white lines indicate the position of the PEM film. Recovery after bleaching (b and g) is shown at 4 s (c and h), 8 s (d and i) and 20 s (e and j). Mean fluorescence intensity profiles obtained by averaging all profiles along the film at different times in FRAP experiments with lysozyme (k) and BSA (l). Analysis according to Seiffert *et al.* by Gaussian fitting. Insets show a square width at half minimum of the Gaussian w^2 as a function of time. Diffusion constants are derived from the slope of the best-fit straight lines (here: lysozyme (4.4 ± 0.9) µm s^{-1}). BSA does not diffuse in the observed time interval (−0.02 µm s^{-1}).

Table 1 Overview of the molecules used for FRAP experiments: molecular masses M_w, isoelectric points pI, hydrodynamic radii R_0 and calculated diffusion coefficients D

Molecule	M_w [Da]	pI (charge sign)	R_0 [nm]	D [µm^2 s^{-1}]
Papain	23 400	8.8 (+)	4.2	2.2 ± 0.2
Lysozyme	14 700	11 (+)	1.9	4.4 ± 0.3
Catalase	250 000	5.4 (−)	5.4	3.9 ± 0.3
Lactalbumin	14 200	4.2 (−)	1.7	0.04 ± 0.01
BSA	66 000	5 (−)	3.6	—
Fluorescein	390	6.4 (−)	0.6	2.1 ± 0.4

However, catalase diffuses about as quickly as papain and lysozyme and two orders of magnitude faster than lactalbumin.

No consistent correlation of D with the size and charge of proteins was found. We conclude that the protein associated with and dissociated from the film is more complex than is reflected in their overall size and charge. For further interpretation, a deeper study will be performed in future. Due to the size-independent exclusion of uncharged polysaccharide molecules, we assume that there is no distinct permanent mesh size in the polymer film. Rather we believe that the proteins interact with freely diffusing PLL molecules as well as HA molecules and move inside dynamic pores in the immobile HA matrix (Scheme 1). These pores appear to have a size in the range of the largest protein tested, catalase (10 nm). This network concept of PEMs is derived from reports stating that HA is immobile[14] while PLL molecules in the film occur in distinct fractions: fast ($D \sim 1$ µm^2 s^{-1}), slow ($D \sim 0.2$ µm^2 s^{-1}) and immobile.[28] HA and the slowly diffusing PLL may form a network, in the mesh of which the fast PLL fraction migrates. The similarity between the PLL diffusion reported earlier and the diffusion coefficients measured here for the proteins papain, lysozyme and catalyse indicates a relation between both. The small negatively charged fluorescein has a D similar to proteins or the fast PLL fraction ((2.1 ± 0.4) µm^2 s^{-1}). It most likely diffuses as quickly as the fast PLL fraction (Table 1) due to binding to PLL driven by electrostatic interactions.

In contrast to the other proteins, BSA does not diffuse to any measurable degree: neither vertically (as shown by its distribution across the film) nor laterally (as shown by the diffusion measurements). However, it adsorbs strongly to the surface of the PEM. In contrast to PLL, HA is immobile in the PEM.[14] This leads to the assumption that BSA adheres to the non-diffusing part of the polymer film. The following arguments support this hypothesis: (a) in spite of its charge, BSA is already known to bind to surfaces of like charge.[37] (b) Insoluble complexes are formed when BSA is mixed with (the negatively charged) HA, as measured turbidimetrically (data not shown). Combinations of the other proteins employed here with

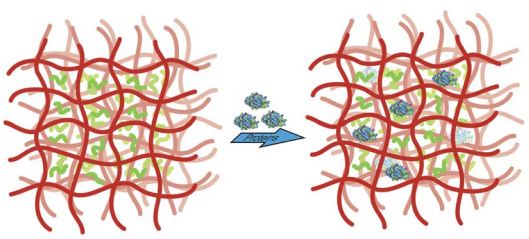

Scheme 1 Scheme of the polymer film made of matrix-forming HA (red) and free diffusing PLL (green). Incubated proteins interact with diffusing PLL molecules as well as HA molecules and move inside dynamic pores in the immobile HA matrix.

This journal is © The Royal Society of Chemistry 2012

either HA or PLL, in contrast, did not lead to an increase in turbidity. The diffusion coefficient of human serum albumin (HSA) in films made of poly(sodium styrene sulfonate) (PSS) and poly(allylamine hydrochloride) (PAH) was reported to be 0.01 $\mu m^2 s^{-1}$ to 0.001 $\mu m^2 s^{-1}$.[38] Hence, we cannot exclude that a very slow diffusion of BSA in the films may have gone unnoticed due to the limited incubation time (45 min). In contrast to our results, Vogt *et al.* observed diffusion of HSA in PEMs of PLL and HA.[32] However, they showed a reduction of the diffusion of HSA with increasing protein concentration from $\sim$60 $\mu m^2 s^{-1}$ for 2 $\mu g ml^{-1}$ (incubation concentration) to less than 0.1 $\mu m^2 s^{-1}$ for 100 $\mu g ml^{-1}$. This concentration still is five times lower than the one we used. If we extrapolate the findings of Vogt *et al.* to our case, the diffusion coefficient would be below the detection limit given by the observation time ($t = 60$ s).

Films made of PLL and HA exhibit large thicknesses. It is, therefore, possible to employ optical microscopy for detecting molecular interactions with the film in a wet state. By using cylindrical glass supports that were viewed from the side, we were able to study for the first time the distribution and diffusion coefficients of molecules as a function of their vertical position in the film (x axis, Fig. 1). Based on the analyses of differently sized and charged proteins, small dye molecules and uncharged macromolecules (dextranes), we believe that the transport in the film is governed by electrostatic interactions between the molecules and the immobile HA matrix and mobile PLL. The mesh size of the HA matrix of the PEM appears to be larger than the diffusing proteins observed (*i.e.* above 10 nm). Our approach to analyze the film structure with a high resolution in both space and time is a powerful technique for understanding molecular interactions in the film.[39] This allows for prediction and optimization of not only the film composition and its properties but also the accessibility of bioactive molecules as well as nano- or microparticles loaded into the film to cells. Our ongoing work focuses on protein functionality and understanding of protein–film interaction as a prerequisite for design of bioactive surfaces and matrixes, for instance artificial extracellular matrices.

Acknowledgements

This work was supported by the Alexander von Humboldt Foundation in the framework of the Sofja Kovalevskaja program and by the DFG grant VO 1716/2-1. NM acknowledges a fellowship from IMPRS on Biomimetic Systems.

References

1 M. Mrksich, *Curr. Opin. Chem. Biol.*, 2002, **6**, 794.
2 Z. Tang, Y. Wang, P. Podsiadlo and N. A. Kotov, *Adv. Mater.*, 2006, **18**, 3203.
3 J. A. Hubbell, *Curr. Opin. Biotechnol.*, 1999, **10**, 123.
4 H. Ai, S. A. Jones and Y. M. Lvov, *Cell Biochem. Biophys.*, 2003, **39**, 23.
5 D. Richard, I. Nguyen, C. Affolter, F. Meyer, P. Schaaf, J.-C. Voegel, D. Bagnard and J. Ogier, *Small*, 2010, **6**, 2405.
6 K. Ren, T. Crouzier, C. Roy and C. Picart, *Adv. Funct. Mater.*, 2008, **18**, 1378.
7 Z.-M. Liu, Q. Gu, Z.-K. Xu and T. Groth, *Macromol. Biosci.*, 2010, **10**, 1043.
8 K. Ren, L. Fourel, C. G. Rouvière, C. Albiges-Rizo and C. Picart, *Acta Biomater.*, 2010, **6**, 4238.
9 G. Weder, O. Guillaume-Gentil, N. Matthey, F. Montagne, H. Heinzelmann, J. Vörös and M. Liley, *Biomaterials*, 2010, **31**, 6436.
10 K. Kirchhof, K. Hristova, N. Krasteva, G. Altankov and T. Groth, *J. Mater. Sci.: Mater. Med.*, 2009, **20**, 897.
11 Z. Song, J. Yin, K. Luo, Y. Zheng, Y. Yang, Q. Li, S. Yan and X. Chen, *Macromol. Biosci.*, 2009, **9**, 268.
12 C. M. Jewell and D. M. Lynn, *Adv. Drug Delivery Rev.*, 2008, **60**, 979.
13 C. Picart, P. Lavalle, P. Hubert, F. J. G. Cuisinier, G. Decher, P. Schaaf and J.-C. Voegel, *Langmuir*, 2001, **17**, 7414.
14 C. Picart, J. Mutterer, L. Richert, Y. Luo, G. D. Prestwich, P. Schaaf, J.-C. Voegel and P. Lavalle, *Proc. Natl. Acad. Sci. U. S. A.*, 2002, **99**, 12531.
15 T. Boudou, T. Crouzier, K. Ren, G. Blin and C. Picart, *Adv. Mater.*, 2010, **22**, 441.
16 S. Pavlukhina and S. Sukhishvili, *Adv. Drug Delivery Rev.*, 2011, **63**, 822.
17 V. Gribova, R. Auzely-Velty and C. Picart, *Chem. Mater.*, 2012, **24**, 854.
18 N. Madaboosi, K. Uhlig, S. Schmidt, M. S. Jäger, H. Möhwald, C. Duschl and D. V. Volodkin, *Lab Chip*, 2012, **12**, 1434.
19 C. Porcel, Ph. Lavalle, G. Decher, B. Senger, J.-C. Voegel and P. Schaaf, *Langmuir*, 2007, **23**, 1898.
20 T. Crouzier, L. Fourel, T. Boudou, C. Albigès-Rizo and C. Picart, *Adv. Mater.*, 2011, **23**, 111.
21 X. Wang and J. Ji, *Langmuir*, 2009, **25**, 11664.
22 D. V. Volodkin, N. Madaboosi, J. Blacklock, A. G. Skirtach and H. Möhwald, *Langmuir*, 2009, **25**, 14037.
23 J. T. Wilson, W. Cui, V. Kozlovskaya, E. Kharlampieva, D. Pan, Z. Qu, V. R. Krishnamurthy, J. Mets, V. Kumar, J. Wen, Y. Song, V. V. Tsukruk and E. L. Chaikof, *J. Am. Chem. Soc.*, 2011, **133**, 7054.
24 A. G. Skirtach, D. V. Volodkin and H. Möhwald, *ChemPhysChem*, 2010, **11**, 822.
25 S. Schmidt, N. Madaboosi, K. Uhlig, D. Köhler, A. Skirtach, C. Duschl, H. Möhwald and D. V. Volodkin, *Langmuir*, 2012, **8**, 3398.
26 D. Volodkin, A. Skirtach and H. Möhwald, *Polym. Int.*, 2012, **61**, 673.
27 D. Volodkin, A. Skirtach and H. Möhwald, *Adv. Polym. Sci.*, 2011, **240**, 135.
28 L. Jourdainne, S. Lecuyer, Y. Arntz, C. Picart, P. Schaaf, B. Senger, J.-C. Voegel, P. Lavalle and T. Charitat, *Langmuir*, 2008, **24**, 7842.
29 L. Shen, P. Chaudouet, J. Ji and C. Picart, *Biomacromolecules*, 2011, **12**, 1322.
30 L. Szyk, P. Schaaf, C. Gergely, J.-C. Voegel and B. Tinland, *Langmuir*, 2001, **17**, 6248.
31 C. Picart, J. Mutterer, Y. Arntz, J.-C. Voegel, P. Schaaf and B. Senger, *Microsc. Res. Tech.*, 2005, **66**, 43.
32 C. Vogt, V. Ball, J. Mutterer, P. Schaaf, J.-C. Voegel, B. Senger and P. Lavalle, *J. Phys. Chem. B*, 2012, **116**, 5269.
33 P. Lavalle, C. Picart, J. Mutterer, C. Gergely, H. Reiss, J. C. Voegel, B. B. Senger and P. Schaaf, *J. Phys. Chem. B*, 2004, **108**, 635.
34 C. Porcel, P. Lavalle, V. Ball, G. Decher, B. Senger, J.-C. Voegel and P. Schaaf, *Langmuir*, 2006, **22**, 4376.
35 J. K. Armstrong, R. B. Wenby, H. J. Meiselman and T. C. Fisher, *Biophys. J.*, 2004, **87**, 4259.
36 S. Seiffert and W. Oppermann, *J. Microsc.*, 2005, **220**, 20.
37 W. Ouyang and M. Müller, *Macromol. Biosci.*, 2006, **6**, 929.
38 L. Szyk, P. Schwinté, J.-C. Voegel, P. Schaaf and B. Tinland, *J. Phys. Chem. B*, 2002, **106**, 6049.
39 R. v. Klitzing, *Phys. Chem. Chem. Phys.*, 2006, **8**, 5012.